Design and Control of Parallel Three Phase Voltage Source Inverters in Low Voltage AC Microgrid

El Hassane MARGOUM[1], *Nissrine KRAMI*[1], *Luis SECA*[2], *Carlos MOREIRA*[2], *Hassan MHARZI*[1]

[1]Department of Electrical Engineering, National School of Applied Science, Ibn Tofail University, Kenitra, Morocco
[2]Institute for Systems and Computer Engineering, Technology and Science (INESC TEC), Faculty of Engineering, University of Porto, R. Dr. Roberto Frias, 4200 Porto, Portugal

margoum.elhassane@gmail.com, nissrine.krami@gmail.com, lseca@inescporto.pt, carlos.moreira@inesctec.pt, h_mharzi@yahoo.fr

DOI: 10.15598/aeee.v15i2.1912

Abstract. *Design and hierarchical control of three phase parallel Voltage Source Inverters are developed in this paper. The control scheme is based on synchronous reference frame and consists of primary and secondary control levels. The primary control consists of the droop control and the virtual output impedance loops. This control level is designed to share the active and reactive power correctly between the connected VSIs in order to avoid the undesired circulating current and overload of the connected VSIs. The secondary control is designed to clear the magnitude and the frequency deviations caused by the primary control. The control structure is validated through dynamics simulations. The obtained results demonstrate the effectiveness of the control structure.*

Keywords

Droop control, energy storage systems, hierarchical control, MicroGrid, Smart grid.

1. Introduction

The MicroGrid (MG) concept has been proposed in order to increase controllability and observability of the distribution grid [1]. Hence, MG can integrate different types of Distributed Generation (DG) such as Renewable Energy Sources (RES) (PhotoVoltaic (PV) panels, micro windturbines), low carbon technologies, Energy Storage Systems (ESS) and loads. All these components are connected together and smartly managed in order to improve reliability and security of supply at the distribution level [1] and [2].

MG is a flexible system [3]. It can operate in two modes: connected to the main network (grid connected mode) at the Low Voltage (LV) level or autonomously (islanded mode) [3]. In the grid connected mode, the MG can exchange the power with the main grid and can also provide ancillary services to the upstream distribution network, such as reactive power, grid frequency support and so forth [4] and [5]. The amount of power exchanged with the external grid is calculated by the tertiary control functions implemented generally in a MicroGrid Central Controller (MGCC) [3], [5], [6] and [7]. In the case of contingencies or faults occurrence in the main grid, the MG changes the mode of operation from grid connected to islanded mode [4], where the power demanded by the local loads is supplied by local distributed generations, since the MG is operating disconnected from the main grid. The Energy Management System (EMS) takes into account the State of Charge (SoC) of ESSs, controllable sources and controllable loads in order to balance generation and consumption, thus improving reliability, efficiency and security of supply [1], [5], [8] and [9].

The MG requirements and the nature of power generated by DGs make the power converters indispensable components. In the case of AC MG, the final stage is an inverter (DC-AC converter). The inverters are very flexible devices that allow implementation of advanced control solutions in order to increase controllability of the MG, thus enabling further integration

of intermittent RES [3], [4], [7] and [10]. The power inverters in AC MG can be classified into grid forming and grid feeding units [4]. The grid forming units operate as Voltage Source Inverters (VSI). They are responsible for regulation of frequency and magnitude of the AC bus voltage. Moreover, they are mandatory when the MG operates in islanded mode, since they are the only ones responsible for the voltage regulation. In contrast, the grid feeding units are designed to inject power into the grid and they are often connected to the DGs based on RES such as PV systems and micro-wind turbines. However, unlike grid forming units, the grid feeding units cannot constitute a MG [4] and [5].

When the MG is operating in the islanded mode, it is necessary to use fast energy storage technologies in order to balance generation and consumption and keep the amplitude and frequency of the common load bus voltage in acceptable limits [10]. The ESS are interfaced by VSIs that are connected in parallel through the MG [1] and [10]. Adequate power sharing is required in order to avoid the undesired circulating current as well as theoverload power converters [3]. Droop control technique has been widely used as an autonomous power sharing solution. This technique is based on local information [3], [4], [5], [7] and [11]. However, it suffers from several drawbacks, especially when it is applied to low voltage grids that have a high R/X ratio due to resistive distribution feeders [3] and [12]. Hence, the active and reactive power are affected by the coupling impedance [13]. An additional control loop called Virtual Output Impedance (VOI) has been proposed [14] and [15], this control loop makes the distribution grid behaving like an inductive grid, thus ensuring the active and reactive power decoupling and improving the system stability. By adding this control loop, the active Power-Frequency (P-ω) and the reactive Power-Voltage (Q-V) can be applied to share the active and reactive power, respectively [4] and [12]. Althoughthe frequency and the voltage are directly involved (frequency and amplitude deviations). For this reason, a centralized controller based on low bandwidth communication links has been proposed in order to restore the frequency and the magnitude to their nominal values [3], [5] and [7].

Hierarchical control structure of MG has been proposed in several works [3], [5], [7] and [16]. This control structure is a compromise between fully centralized and fully decentralized approaches [5]. It includes three main control levels: primary, secondary and tertiary control [3] and [7]. The primary control is responsible for power sharing between the connected inverters in order to avoid the undesired circulating current and converters overload. The secondary control restores the amplitude and the frequency deviations of the load bus voltage caused by the power sharing controller. The tertiary control manages the power between the MG and the main grid [3].

Primary and secondary control for parallel connected VSIs forming an autonomous AC MG are developed and discussed in this paper. The control scheme consists of a local controller and a centralized controller. The local controller includes voltage and current Proportional Integral (PI) controllers based on synchronous reference frame and power sharing controller that consists of droop control and VOI. The secondary control implemented in a centralized controller restores the deviations produced by the power sharing controller.

The remainder of this paper is structured as follows: Section 2. presents a design of the MG local controller that consists of inner loops, droop control and virtual output impedance. Section 3. presents a design of the centralized secondary control. Simulation results for two parallel connected VSIs forming an islanded AC MG are presented and discussed in Sec. 4.

2. Local Controller Design: Inner Loops and Primary Control

The VSIs local controller is based on local measurements [3], it generally includes droop control, output virtual impedance and inner control loops (Voltage and current loops) [3], [7], [13], [17] and [18]. The block diagram of the VSI local controller is depicted in Fig. 1. The power stage of each VSI consists of a three-leg three phase inverter connected to a Battery Energy Storage System (BESS) through the DC link Capacitor (C), loaded by an LC filter and connected to the MG AC bus through a line impedance.

The VSI control system consists of the power sharing controller (droop control and VOI), voltage loop, current loop and the Pulse Width Modulator (PWM). The park transformation is used to transform variables from the natural frame to the synchronous reference frame. More details are presented in the following subsections.

2.1. Inner Loops

The VSIs inner control loops are based on synchronous reference frame including an outer voltage loop and an inner current loop as shown in Fig. 2. Proportional-Integral (PI) controllers are used in two control loops [19]. Voltage and current feed-forward have been added in order to improve performances of the regulators [5].

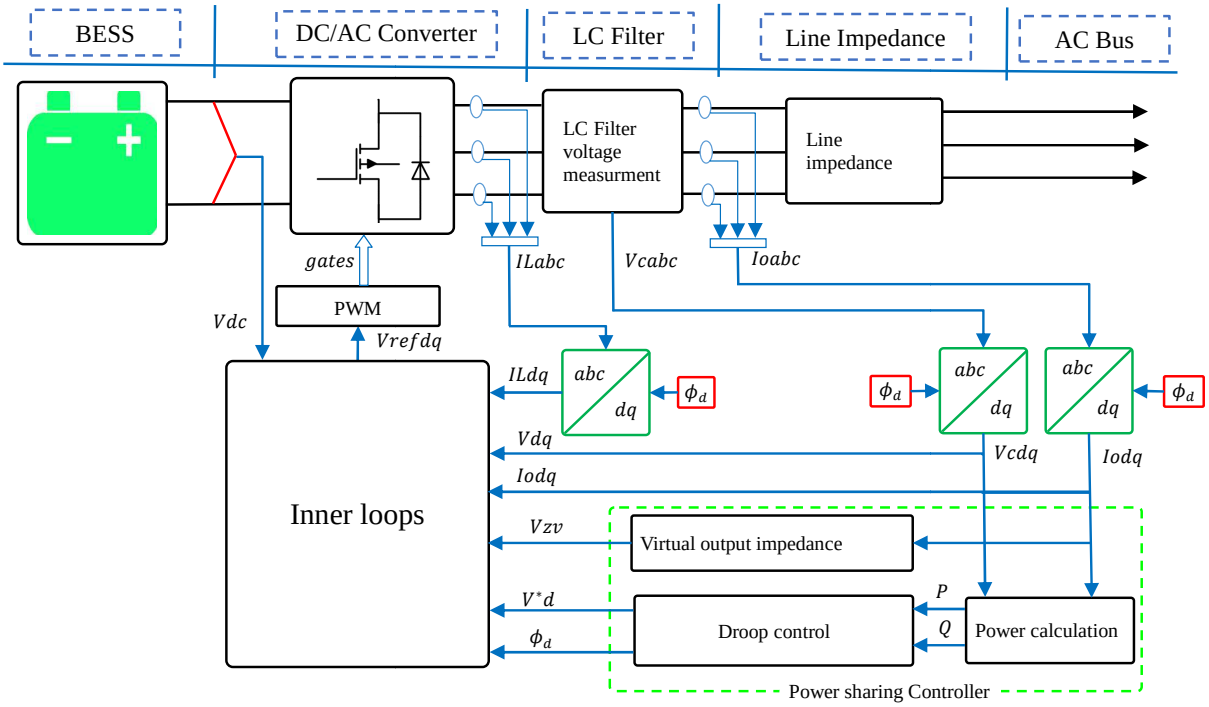

Fig. 1: VSI local controller.

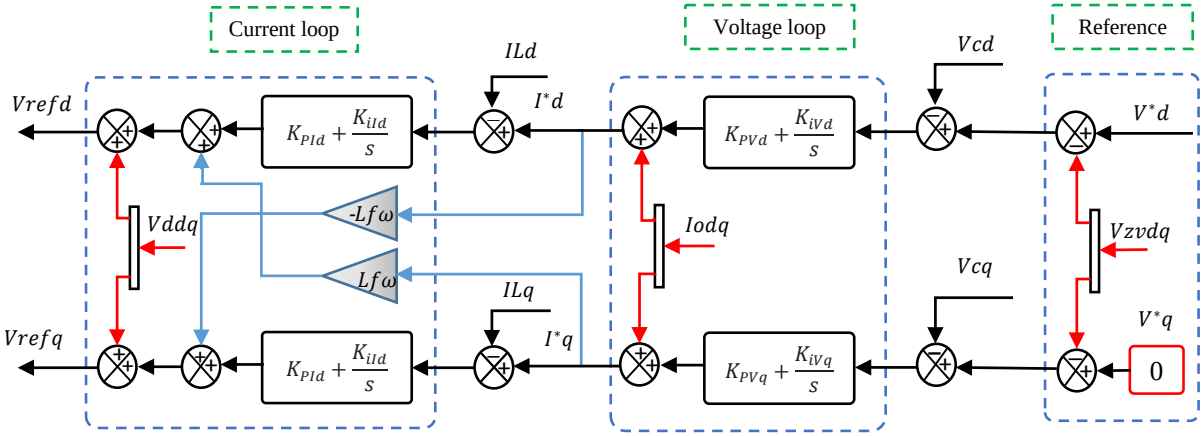

Fig. 2: VSI inner control loops.

Transfer functions of the voltages (V_d and V_q) and currents (I_d and I_q) controllers are given as follows [19]:

$$R_{Vd}(s) = K_{PVd} + \frac{K_{iVd}}{s}, \tag{1}$$

$$R_{Vq}(s) = K_{PVq} + \frac{K_{iVq}}{s}, \tag{2}$$

$$R_{Id}(s) = K_{PId} + \frac{K_{iId}}{s}, \tag{3}$$

$$R_{Iq}(s) = K_{PIq} + \frac{K_{iIq}}{s}, \tag{4}$$

where K_{PVd} (K_{PVq}) are proportional term coefficients of the direct (quadrature) voltage controller, and K_{iVd} (K_{iVq}) are integral term coefficients of the direct (quadrature) voltage controller.

K_{PId} (K_{PIq}) are proportional term coefficients of the direct (quadrature) current controller, and K_{iId} (K_{iIq}) are integral term coefficients of the direct (quadrature) current controller. A block diagram of the local controller is depicted in Fig. 2.

2.2. Primary Control

If two or more power converters are parallel connected to a common Load Bus (LB), the undesired circulating current can appear and the power will not be shared properly between the parallel connected power converters [3]. In order to solve this power sharing issue, the primary control has been proposed [3]. This control level adapts the frequency and the amplitude of the

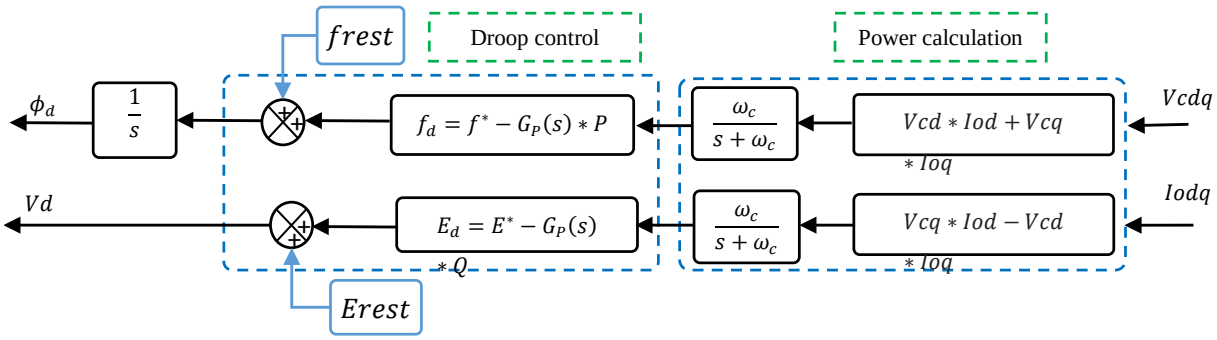

Fig. 3: Block diagram of power calculation and droop control.

voltage reference in order to share the active and reactive power properly between the connected VSIs. Thus avoiding the undesired circulating current and the converters overload [3], [4] and [7]. This control level consists of droop control and the VOI [3].

1) Power Calculation and Droop Control

The equations of active and reactive power generated by a VSI are given in dq-coordinates variables by Eq. (5) and Eq. (6), respectively [4].

$$P = \frac{3}{2}\left(V_{cd} \cdot I_{od} + V_{cq} \cdot I_{oq}\right), \tag{5}$$

$$Q = \frac{3}{2}\left(V_{cq} \cdot I_{od} - V_{cd} \cdot I_{oq}\right), \tag{6}$$

where $Vcdq$ and $Iodq$ are the capacitor voltage and the current after the LC filter.

A block diagram of the power calculation and droop control is shown in Fig. 3.

The Park transformation is used to obtain the dq-coordinates variables.

$$\begin{bmatrix} Xd \\ Xq \\ X0 \end{bmatrix} = \\ = \frac{2}{3}\begin{bmatrix} \cos(\theta) & \cos(\theta - \frac{2\pi}{3}) & \cos(\theta + \frac{2\pi}{3}) \\ \sin(\theta) & \sin(\theta - \frac{2\pi}{3}) & \sin(\theta + \frac{2\pi}{3}) \\ \frac{1}{2} & \frac{1}{2} & \frac{1}{2} \end{bmatrix} \begin{bmatrix} Xa \\ Xb \\ Xc \end{bmatrix}, \tag{7}$$

where $(Xd, Xq, X0)$ is the variable vector in synchronous reference frame and (Xa, Xb, Xc) is the variable vector in the natural reference frame.

In order to filter the active and reactive power ripples a first order Low Pass Filter (LPF) is used. The transfer function of the LPF is given by Eq. (8):

$$LPF(s) = \frac{\omega_c}{s + \omega_c}, \tag{8}$$

where ω_c is the LPF cut-off frequency.

A MG consists of a number of parallel connected converters [11]. Figure 4 shows the equivalent circuit of

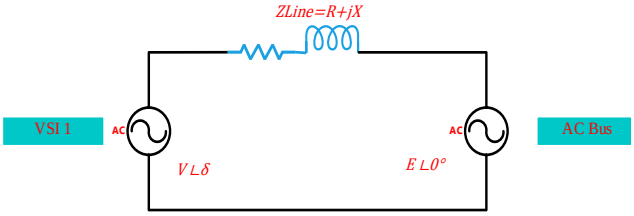

Fig. 4: Equivalent circuit of two parallel connected VSIs.

a VSI connected in parallel with an AC bus. The active and reactive power delivered by the VSI are expressed as follows [20]:

$$P = \left(\frac{EV}{Z}\cos\delta - \frac{V^2}{Z}\right)\cos\theta + \frac{EV}{Z}\sin\delta \cdot \sin\theta, \tag{9}$$

$$Q = \left(\frac{EV}{Z}\cos\delta - \frac{V^2}{Z}\right)\sin\theta - \frac{EV}{Z}\sin\delta \cdot \cos\theta, \tag{10}$$

where V and E are the VSI voltage amplitude and AC bus voltage amplitude, respectively, Z and θ are the amplitude and the angle of the line impedance, respectively, δ is the load angle.

When the coupling impedance is mainly inductive, the active and reactive power equations become as follows:

$$P \approx \frac{EV}{X}\sin\delta, \tag{11}$$

$$Q \approx \frac{EV}{X}\cos\delta - \frac{V^2}{X}. \tag{12}$$

Low voltage grids have a high $\frac{R}{X}$. In this work we have used the VOI to ensure the inductive behavior of the line impedance. We assumed that the equivalent line impedance is mainly inductive.

The frequency and voltage droop expressions are given by Eq. (13) and Eq. (14), respectively:

$$f_d = f_{ref} - G_P(S) \cdot P, \tag{13}$$

$$E_d = E_{ref} - G_Q(S) \cdot Q. \tag{14}$$

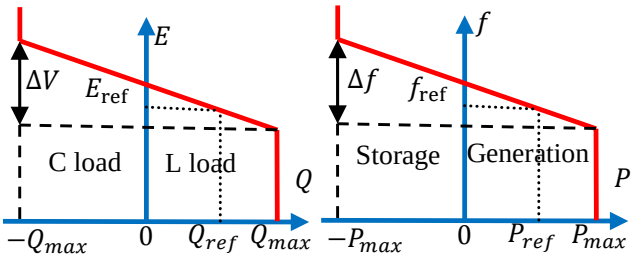

Fig. 5: Frequency (a) and voltage (b) droop characteristics for inductive line impedance.

These equations are graphically presented as depicted in Fig. 5.

Where E_{ref} and f_{ref} are the voltage magnitude and frequency reference, respectively, E_d, f_d and ϕ_d are the drooped voltage magnitude, frequency and the phase reference, respectively, P and Q are the measured active and reactive power.

$G_P(s)$ and $G_P(s)$ can be designed as follows:

$$G_P(s) = Kp = \frac{\Delta f}{P_{\max}}, \tag{15}$$

$$G_q(s) = Kq = \frac{\Delta E}{2Q_{\max}}, \tag{16}$$

where Kp and Kq are the proportional coefficients of the frequency and the voltage droop, respectively, Δf and ΔE are the maximum acceptable deviation of the frequency and the voltage, respectively, $P_{\max}$ and $Q_{\max}$ are the maximum active and reactive power delivered by the VSI, respectively.

2) Virtual Output Impedance (VOI)

When the coupling impedance is not purely inductive, the traditional droop control scheme cannot be applied directly. However, the droop control is not enough to ensure the system stability and reactive power sharing between the connected VSIs. For this reason, a virtual impedance loop was proposed in the technical literature [3], [11], [12], [13], [15], [21], [22] and [23]. The objective of this control loop is to decouple active and reactive power control [4] and [24], thus ensuring the system stability and improving the performances of the droop control without causing any power losses.

The VOI loop consists of dropping the voltage reference calculated by the droop control loop proportionally to the output current. The dropped voltage reference is expressed as follows:

$$V_{ref} = V_d - Z_v(s) \cdot I_o, \tag{17}$$

where $Z_v(s)$ is the VOI transfer function, V_d voltage reference calculated by the droop control loop and I_o is the output current after the LC filter.

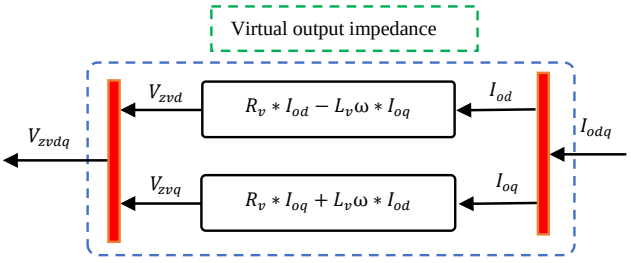

Fig. 6: Synchronous reference frame virtual output impedance.

The synchronous reference frame VOI depicted in Fig. 6 is adopted in this work. The VOI equations are given in dq-coordinates as follows [12] and [24]:

$$V_{zvd} = R_v \cdot I_{od} - L_v\omega \cdot I_{oq}, \tag{18}$$

$$V_{zvq} = R_v \cdot I_{oq} + L_v\omega \cdot I_{od}, \tag{19}$$

where R_v and L_v being the virtual resistance and the virtual inductance and I_odq is the dq-coordinates output current of the VSI after the LC filter (as shown in Fig. 1).

The virtual resistance has been added in order to damp the oscillations [22]. As the virtual inductance is high as good power sharing performances are achieved. However, its size is limited by the maximum voltage deviations in the LB. Since, the VOI drops the voltage reference generated by the droop control loop proportionally to the output current.

3. Centralized Controller Design: Secondary Control

Droop control and virtual output impedance control loop produce voltage and frequency deviations. The secondary control is designed to restore these deviations and keep the frequency and the amplitude at the LB in the allowable limits [3] and [6]. The secondary controller is based on two PI controllers, one restores the voltage deviations and the other one restores the frequency deviations. The secondary control block diagram is depicted in Fig. 7.

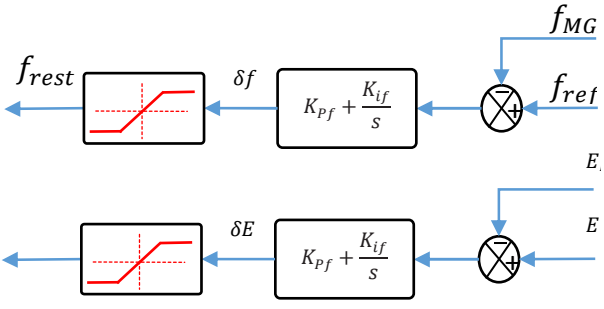

Fig. 7: Block diagram of Secondary control level.

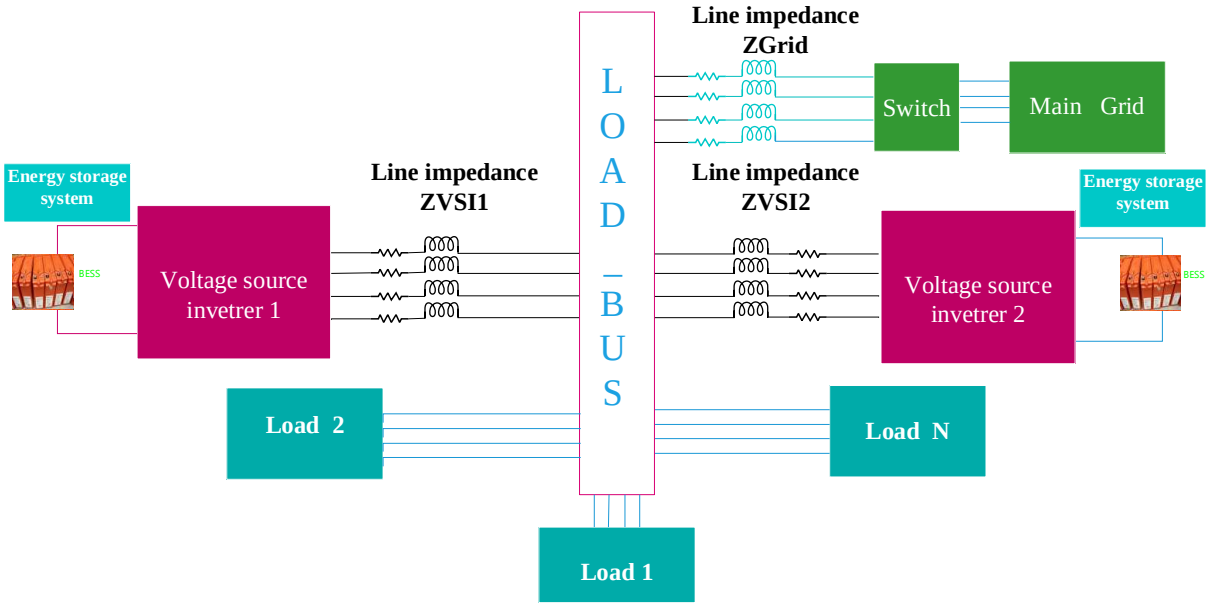

Fig. 8: Block diagram of two parallel connected VSIs with distributed loads forming an AC MicroGrid.

The voltage and frequency restoration signals can be calculated as follows [3]:

$$\delta f = k_{pf}(f^*_{MG} - f_{MG}) + k_{if}\int(f^*_{MG} - f_{MG})\mathrm{d}t, \quad (20)$$

$$\delta E = \\ = k_{pE}(E^*_{MG} - E_{MG}) + k_{iE}\int(E^*_{MG} - E_{MG})\mathrm{d}t, \quad (21)$$

where δf (δE) are the frequency (amplitude) restoration signals, f^*_{MG} (E^*_{MG}) and f_{MG} (E_{MG}) are the reference of the frequency (amplitude) and the measured frequency (amplitude) at the LB, respectively, K_{Pf} (K_{PE}) are the proportional term coefficients of the frequency (voltage) PI controller, and K_{if} (K_{iE}) are the integral term coefficients of the frequency (amplitude) PI controller, respectively.

4. Simulation Results

In order to evaluate the control system performances, an islanded MG formed by two parallel connected VSIs, as shown in Fig. 8, are simulated using Matlab/Simulink environment. Each inverter is connected to the LB through a line impedance, the output impedance of two VSIs are not equal, ZVSI2= 2·VSI1 as seen in Fig. 8. The system parameters are listed in Tab. 1 The switching frequency of the VSIs is set to 20 kHz. In order to show clearly the active and reactive power sharing between the connected converters at different load conditions, three loads are connected to the load bus at different times (unbalanced loads are not considered in this study). Figure 9 shows the power sharing between the VSIs. After the connection of load 1 to the LB from $t = 0$ s to $t = 5$ s, the active power is shared properly between the VSIs and the reactive power is shared with a small error. Then, load 2 is connected at $t = 5$ s, and disconnected at $t = 10$ s. Meanwhile, the active power at the LB increases from 5 kW to 10 kW. As a consequence, the reactive power error between the two VSIs increases. This error is due to the strong coupling between the active and reactive power. At $t = 15$ s, the second VSI is disconnected from the LB and thenthe connected loads are supplied by one VSI. At $t = 17$, another active load of 1 kW is connected to the LB. Figure 10 shows the output voltage at the LB. Figure 11 and Fig. 12 show the output current of VSI1 and VSI2, respectively.

The main disadvantage of the droop control is the steady state voltage and frequency deviations, the power sharing is achieved through dropping the amplitude and the frequency of the voltage. Figure 13 shows the nominal and measured values of the frequency of the load bus voltagethat drops proportionally to the active power. Figure 14 shows the nominal voltage (220 V) and the load bus voltage, the load bus voltage drops proportionally to the reactive power.

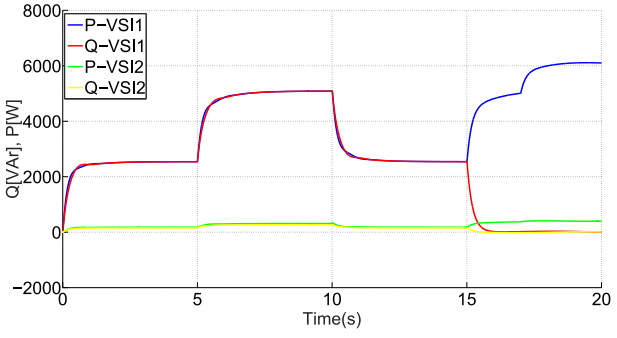

Fig. 9: Active and reactive power sharing.

Tab. 1: System parameters.

Power stage			
Parameter		**Value**	
Nominal RMS voltage: V_{rms} (V)		220	
Nominal frequency: f (Hz)		50	
DC voltage: V_{dc} (V)		650	
Inverter filter inductance: L_f (H)		2.0E-3	
Inverter filter capacitance: C_f (F)		11.0E-6	
VSI 1 line impedance: ZVSI1=R1+jX1		0.2+j0.0126	
VSI 2 line impedance: ZVSI2=R2+jX2		0.4+j0.0252	
load 1: P (kW), Q (KVAR)		P=5, Q=250	
load 2: P (kW), Q (KVAR)		P=5	
load 3: P (kW), Q (KVAR)		P=1	
Inner loops			
Voltage controller PI		**Current controller PI**	
KpVd = 0.5, KiVd = 1000, KpVq = 0.15, KiVq = 300.		KpId = 40, KiId = 85, KpIq = 40, KiIq = 85.	
Primary control			
Droop control		**Virtual output impedance**	
Kp=3.33E-5	Kq=22E-3	Rv=1Ω	Lzv=7 mH
Secondary control			
Frequency restoration		**Voltage restoration**	
Kpf=15E-4	Kif=500	KpE=15E-4	KiE=1000

Power calculation filters: $T = 0.2$

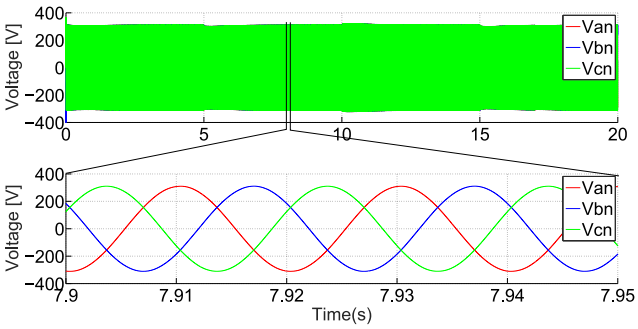

Fig. 10: Output voltage of a VSI.

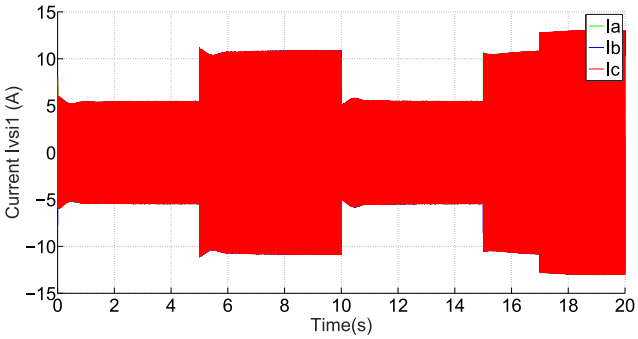

Fig. 11: Output current of a VSI1.

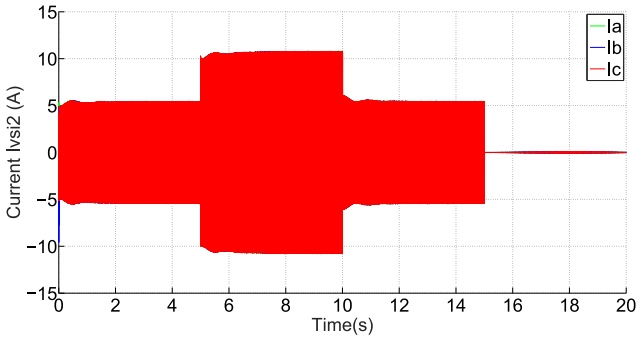

Fig. 12: Output current of a VSI2.

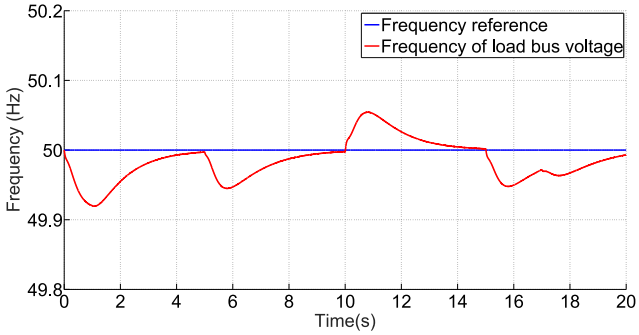

Fig. 13: Frequency reference and LB frequency without secondary control.

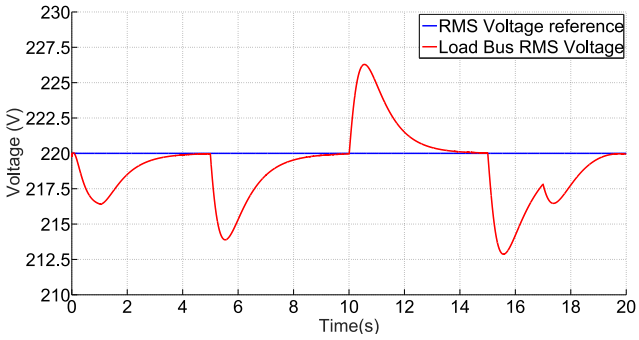

Fig. 14: RMS voltage reference and LB RMS voltage without secondary control.

In order to keep the frequency and the amplitude of the load bus voltage in acceptable limits, the secondary control is used. Figure 15 and Fig. 16 show the reference and the measured frequency and voltage in the LB respectively. The secondary control restores correctly the deviations produced by the primary control. The frequency and RMS voltage of the LB are kept in the allowable limits.

The load bus frequency and voltage overshoots in Fig. 15 and Fig. 16 are causedby the disconnection of load 2 at $t = 10$ s, the secondary control regulated the voltage and the frequencyto their nominal values.

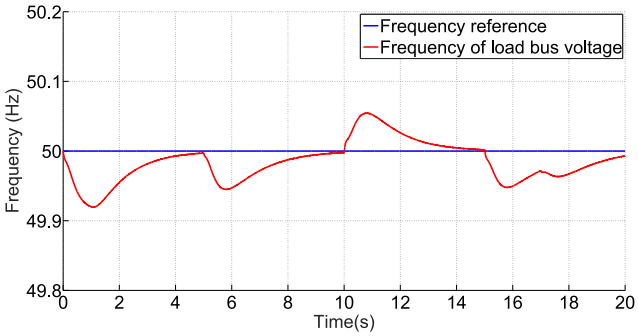

Fig. 15: Frequency reference and LB frequency with secondary control.

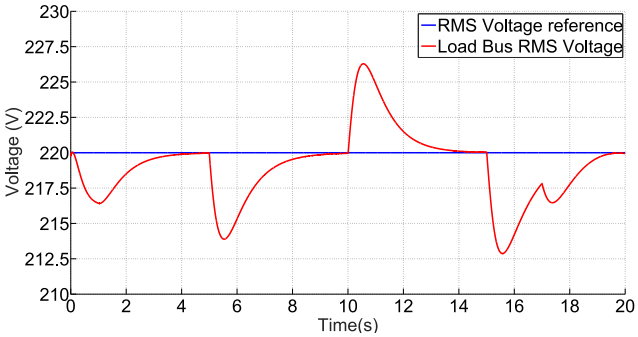

Fig. 16: RMS voltage reference and LB RMS voltage with secondary control.

5. Conclusion

Design and analysis of inner control loops, Primary and secondary control for parallel connected VSIs forming a low voltage MG are presented in this paper. The inner control loops are based on synchronous reference frame. PI controllers are used in voltage and current loops. The primary control includes droop control and a VOI loop. The centralized secondary control includes voltage and frequency restoration controllers.

The simulation results are also presented and show that the active and reactive power are shared properly. The amplitude and the frequency of the LB voltage are restored by the centralized secondary control and kept in the allowable limits.

Acknowledgment

This work was supported by IRESEN (Institut de Recherche en Energie Solaire et Energies Nouvelles) of Morocco in the framework of the Inno-PV research project "SECRETS - Sustainable Energy Clusters REalized Through Smart Grids".

References

[1] GOUVEIA, C., J. MOREIRA, C. L. MOREIRA and J. A. PECAS LOPES. Coordinating storage and demand response for microgrid emergency operation. *IEEE Transactions on Smart Grid.* 2013, vol. 4, iss. 4, pp. 1898–1908. ISSN 1949-3053. DOI: 10.1109/TSG.2013.2257895.

[2] BLAABJERG, F. and J. M. GUERRERO. Smart Grid and Renewable Energy Systems. In: *International Conference on Electrical Machines and Systems.* Beijing: IEEE, 2011, pp. 1–10. ISBN 978-1-4577-1044-5. DOI: 10.1109/ICEMS.2011.6073290.

[3] GUERRERO, J. M., J. C. VASQUEZ, J. MATAS, L. G. DE VICUNA and M. CASTILLA. Hierarchical control of droop-controlled AC and DC microgrids - A general approach toward standardization. *IEEE Transactions on Industrial Electronics.* 2011, vol. 58, iss. 1, pp. 158–172. ISSN 0278-0046. DOI: 10.1109/TIE.2010.2066534.

[4] ROCABERT, J., A. LUNA, F. BLAABJERG and P. RODRIGUEZ. Control of Power Converters in AC Microgrids. *IEEE Transactions on Power Electronics.* 2012, vol. 27, iss. 11, pp. 4734–4749. ISSN 0885-8993. DOI: 10.1109/TPEL.2012.2199334.

[5] DANIEL, E. O., A. MEHRIZI-SANI, A. H. ETEMADI, C. A. CANIZARES, R. IRAVANI, M. KAZERANI, A. H. HAJIMIRAGHA, O. GOMIS-BELLMUNT, M. SAEEDIFARD, R. PALMA-BEHNKE, G. A. JIMENEZ-ESTEVEZ and N. D. HATZIARGYRIOU. Trends in Microgrid Control. *IEEE Transactions on Smart Grid.* 2014, vol. 5, iss. 4, pp. 1905–1919. ISSN 1949-3053. DOI: 10.1109/TSG.2013.2295514.

[6] MENG, L., M. SAVAGHEBI, F. ANDRADE, J. C. VASQUEZ, J. M. GUERRERO and M. GRAELLS. Microgrid central controller development and hierarchical control implementation in the intelligent microgrid lab of Aalborg University. In: *Applied Power Electronics Conference and Exposition.* Charlotte: IEEE, 2015, pp. 2585–2592. ISBN 978-1-4799-6736-0. DOI: 10.1109/APEC.2015.7104716.

[7] VASQUEZ, J. C., J. M. GUERRERO, J. MIRET, M. CASTILLA and L. GARCIA DE VICUNA. Hierarchical Control of Intelligent Microgrids. *IEEE Industrial Electronics Magazine.* 2010, vol. 4, no. 4, pp. 23–29. ISSN 1932-4529. DOI: 10.1109/MIE.2010.938720.

[8] LOPES, J. A. P., C. L. MOREIRA and A. G. MADUREIRA. Defining control strategies for

microgrids islanded operation. *IEEE Transactions on Power Systems.* 2006, vol. 21, iss. 2, pp. 916–924. ISSN 0885-8950. DOI: 10.1109/TPWRS.2006.873018.

[9] GOUVEIA, C., C. L. MOREIRA, J. ABEL, P. LOPES and D. VARAJAO. Microgrid Service Restoration: the role of plugged-in electric vehicles. *IEEE Industrial Electronics Magazine.* 2013, vol. 7, iss. 4, pp. 26–41. ISSN 1932-4529. DOI: 10.1109/MIE.2013.2272337.

[10] WU, D., F. TANG, T. DRAGICEVIC, J. C. VASQUEZ and J. M. GUERRERO. Autonomous Active Power Control for Islanded AC Microgrids With Photovoltaic Generation and Energy Storage System. *IEEE Transactions on Energy Conversion.* 2014, vol. 29, iss. 4, pp. 882–892. ISSN 0885-8969. DOI: 10.1109/TEC.2014.2358612.

[11] VASQUEZ, J. C., J. M. GUERRERO, M. SAVAGHEBI and R. TEODORESCU. Modeling, analysis, and design of stationary reference frame droop controlled parallel three-phase voltage source inverters. *IEEE Transactions on Industrial Electronics.* 2011, vol. 60, iss. 4, pp. 272–279. ISSN 0278-0046. DOI: 10.1109/TIE.2012.2194951.

[12] HE, J. and Y. W. LI. Analysis and design of interfacing inverter output virtual impedance in a low voltage microgrid. In: *IEEE Energy Conversion Congress and Exposition.* Atlanta: IEEE, 2010, pp. 2857–2864. ISBN 978-1-4244-5286-6. DOI: 10.1109/ECCE.2010.5618181.

[13] GUAN, Y., J. M. GUERRERO, X. ZHAO, J. C. VASQUEZ and X. GUO. A New Way of Controlling Parallel-Connected Inverters by Using Synchronous Reference Frame Virtual Impedance Loop - Part I: Control Principle. *Power Electron.* 2016, vol. 31, iss. 6, pp. 4576–4593. ISSN 0885-8993. DOI: 0.1109/TPEL.2015.2472279.

[14] WANG, X., F. BLAABJERG and Z. CHEN. An improved design of virtual output impedance loop for droop-controlled parallel three-phase voltage source inverters. In: *IEEE Energy Conversion Congress and Exposition (ECCE).* Raleigh: IEEE, 2012, pp. 2466–2473. ISBN 978-1-4673-0802-1. DOI: 10.1109/ECCE.2012.6342404.

[15] GUERRERO, J. M., L. GARCIADEVICUNA, J. MATAS, M. CASTILLA and J. MIRET. Output Impedance Design of Parallel-Connected UPS Inverters With Wireless Load-Sharing Control. *IEEE Transactions on Industrial Electronics.* 2005, vol. 52, iss. 4, pp. 1126–1135. ISSN 0278-0046. DOI: 10.1109/TIE.2005.851634.

[16] PALIZBAN, O. and K. KAUHANIEMI. Hierarchical control structure in microgrids with distributed generation: Island and grid-connected mode. *Renewable and Sustainable Energy Reviews.* 2015, vol. 44, iss. 1, pp. 797–813. ISSN 1364-0321. DOI: 10.1016/j.rser.2015.01.008.

[17] BIDRAM, A. and A. DAVOUDI. Hierarchical structure of microgrids control system. *Smart Grid.* 2012, vol. 3, iss. 4, pp. 1963–1976. ISSN 1364-0321. DOI: 10.1109/TSG.2012.2197425.

[18] SAVAGHEBI, M., J. M. GUERRERO, A. JALILIAN and J. C. VASQUEZ. Hierarchical control scheme for voltage unbalance compensation in islanded microgrids. In: *37th Annual Conference of the IEEE Industrial Electronics Society.* Melbourne: IEEE, 2011, pp. 3158–3163. ISBN 978-1-61284-972-0. DOI: 10.1109/IECON.2011.6119815.

[19] BLAABJERG, F., R. TEODORESCU, M. LISERRE and A. V. TIMBUS. Overview of control and grid synchronization for distributed power generation systems. *IEEE Transactions on Industrial Electronics.* 2006, vol. 53, iss. 5, pp. 1398–1409. ISSN 0278-0046. DOI: 10.1109/TIE.2006.881997.

[20] GUERRERO, J. M., J. MATAS, L. G. DE VICUNA, M. CASTILLA and J. MIRET. Wireless-control strategy for parallel operation of distributed-generation inverters. In: *Proceedings of the IEEE International Symposium on Industrial Electronics.* Dubrovnik: IEEE, 2005, pp. 845–850. ISBN 0-7803-8738-4. DOI: 10.1109/ISIE.2005.1529025.

[21] GUERRERO, J. M., M. CHANDORKAR, T.-L. LEE and P. C. LOH. Advanced Control Architectures for Intelligent Microgrids Part I: Decentralized and Hierarchical Control. *IEEE Transactions on Industrial Electronics.* 2013, vol. 60, no. 4, pp. 1254–1262. ISBN 0278-0046. DOI: 10.1109/TIE.2012.2196889.

[22] GUERRERO, J. M., J. MATAS, L. GARCIA DE VICUNA, M. CASTILLA and J. MIRET. Decentralized Control for Parallel Operation of Distributed Generation Inverters Using Resistive Output Impedance. *IEEE Transactions on Industrial Electronics.* 2007, vol. 54, iss. 2, pp. 994–1004. ISSN 0278-0046. DOI: 10.1109/TIE.2007.892621.

[23] WANG, X., Y. W. LI, F. BLAABJERG and P. C. LOH. Virtual-impedance-based control for voltage-source and current-source converters. *IEEE Transactions on Power Electronics.* 2015,

vol. 30, iss. 12, pp. 7019–7037. ISSN 0885-8993. DOI: 10.1109/TPEL.2014.2382565.

[24] SUMMERS, C. D., T. J. BETZ, R. E. MOORE and T. G. TOWNSEND. Implementing the virtual output impedance concept in a three phase system utilising cascaded PI controllers in the dq rotating reference frame for microgrid inverter. In: *Power Electronics and Applications.* Lille: IEEE, 2013, pp. 1–10. ISBN 978-1-4799-0116-6. DOI: 10.1109/EPE.2013.6634691.

About Authors

El Hassane MARGOUM received the M.Sc. degree in electrical engineering from the Higher Normal School of Technical Education, Mohamed V University, Rabat, Morocco in 2014. He is currently pursuing his Ph.D. degree at National school of applied sciences /University of Ibn-Tofail, Kenitra, Morroco. He is working on the SECRETS project (Sustainable Energy Clusters Realized Through Smart Grids) in the development of smart power electronic converters for microgeneration systems, and he is a guest Ph.D. student at the Smart Grids with the Electric Vehicles Laboratory of the Institute for Systems and Computer Engineering (INESC), Porto.

Nissrine KRAMI has been an assistant professor in the Department of Electrical Engineering of the national school of applied sciences of the University of Ibn Tofail since 2010. His research interests are focused on microgrid dynamics and control, smart grids.

Carlos Leal MOREIRA received the B.Sc. and Ph.D. degrees in electrical engineering from the University of Porto, Portugal, in 2003 and 2008, respectively. Since 2010, he has been the smart grid area leader in the Power Systems Unit of the Institute for Systems and Computer Engineering of Porto (INESC Porto). He has also been an assistant professor in the Department of Electrical Engineering of the Faculty of Engineering of the University of Porto since 2008. His research interests are focused on MicroGrid dynamics and control, smart grids, and smart metering.

Luis SECA received the Electrical Engineering degree (five-year course) and the M.Sc. degree (two-year course) in electrical engineering, both from FEUP, in 2002 and 2006, respectively. He is currently a senior Researcher/Consultant in the Power Systems Unit of INESC Porto. His current research interests include steady-state and dynamic studies on integration of distributed energy resources in transmission and distribution networks, voltage and frequency control, and ancillary services provision.

Hassan MHARZI he is professor research at the National School of Applied Sciences, Kenitra, Morocco. Member of the Laboratory for Systems Engineering and Head of Team: Intelligent Energy, Power and Industrial Systems (Eisei). Nantes in France since 1996 and has the ability to supervise research since 2004. His research interests are focused on development and characterization of semiconductor materials for the production of electronic components (diodes, transistors, ptohovoltaic, cells, etc.).